Available online at www.sciencedirect.com
SCIENCE DIRECT®
Polymer 45 (2004) 1235–1242
polymer
www.elsevier.com/locate/polymer

Step-scan alternating DSC study of melting and crystallisation in poly(ethylene oxide)

Krzysztof Pielichowski*, Kinga Flejtuch, Jan Pielichowski

Department of Chemistry and Technology of Polymers, Cracow University of Technology, ul. Warszawska 24, 31-155 Krakow, Poland

Received 29 January 2003; received in revised form 9 December 2003; accepted 17 December 2003

Abstract

Step-scan alternating differential scanning calorimetry (SSA-DSC) method was applied to investigate the phase behaviour of well-characterised poly(ethylene oxide) (PEO). Influence of the three main measurement's parameters of SSA-DSC method: length of the isothermal segment (t_{iso}/s), temperature jump between two subsequent isothermal segments (step/deg) and linear heating rate in dynamic segments (b/K/min), on the shape of reversing and non-reversing components during the melting and crystallisation of PEO, has been evaluated. It was found that the reversing component during melting of PEO is increasing with an increase of the isothermal segment length. This effect is due to the existence of defected polymer crystal structures that form metastable regions between crystal phase and already melted polymer. Reversible recrystallisation in the presence of still existing polymer crystals is facilitated by longer isothermal segments. By increasing the step, the equilibrium of reversible processes is shifted towards products and activation of rate-controlled processes takes place; molecular nucleation is hampered and partial melting and/or recrystallisation proceed slower—this effect can be observed as a decrease of reversing signal with increasing step.

Keywords: Poly(ethylene oxide); Melting; Crystallisation

1. Introduction

Poly(ethylene oxide) (PEO) is an important semi-crystalline polymer which is used in water paints, paper coatings, textile fibres, as a component of packaging materials and as solubilising agent for drugs [1,2]. PEO is among the first and most studied polymers for polymer solid electrolytes that are applied in solid-state batteries [3], capacitors [4] and electrochromic devices [5,6]. A relatively new application that is considered as a very promising one concerns PEO as a thermal energy storage material since it has large heat of fusion and a congruent melting behaviour [7,8]. Its phase behaviour should be considered in terms of both the conformation of individual molecules in the crystalline state and the arrangement of those molecules into micro- and macroscopic structures. In the crystalline state, PEO chain (which has dihedral symmetry, two-fold axes, one passing through the oxygen atoms and the other bisecting the carbon–carbon bond) contains seven structural units and two helical turns per fiber identity period of 19.3 Å—on melting, this helical structure is lost and a liquid containing random coils is obtained [9]. In the crystal lattice, PEO is arranged in form of lamellae and the chains are either in an extended or folded forms [10]. Avrami theory [11] and Lauritzen–Hoffman–Miller [12,13] approach were used for studying the crystallisation behaviour of PEO; Godovsky et al. [14] measured the temperature dependence of the isothermal growth rates of spherulites and overall kinetics of crystallisation—for PEO with average molecular weight of 4000 a minimum in the crystallisation rate was found which was ascribed to the transition from extended to folded chain. The most important discovery from a series of works of Kovacs et al. was the recognition that PEO chains integrally fold when incorporated into crystals, as evidenced by quantized changes of the lamellar thickness with varying crystallisation conditions [15–17]. Cheng et al. [18] applied both nucleation theory and molecular considerations to explain the course of crystallisation of PEO followed by polarised light microscope. They suggested that with increasing molecular length attachment of extended chain

* Corresponding author. Tel.: +48-126282727; fax: +48-126282038.
E-mail address: kpielich@usk.pk.edu.pl (K. Pielichowski).

0032-3861/$ - see front matter © 2003 Elsevier Ltd. All rights reserved.
doi:10.1016/j.polymer.2003.12.045

conformations onto a crystal surface becomes increasingly difficult-attachments with non-integral folded chain conformations are more favourable and the final extended chain crystal may form through an isothermal thickening process on the crystal surface during growth. More recent observations of the spherulite growth rates of PEO indicated that there is some uncertainty of the crystallisation regime since a change in morphology (crystallographic orientation of the growth front) may overlap with a regime II–III transition [19]. In that respect, the kinetic nucleation theory offers a promising framework for describing and understanding isothermal crystallisation rates for linear polymers in quiscent melts or dilute solutions [13]. There are three regimes of crystal growth, which are controlled by competing nucleation and growth processes. Hence, the first regime describes a single nucleation per substrate length, L, where the nucleation rate, i, is slower than the substrate completion rate, g. The crystal growth rate is given by $G_I = biL$, where b is the thickness of a crystalline stem. In the second regime (II), multiple nucleation occurs on the growth face as the nucleation rate is roughly equivalent to or greater than the substrate completion rate. The crystal growth rate follows the equation of $G_{II} = b(2ig)^{1/2}$. The final regime (III) is a state of rapid polynucleation growth where nucleation occurs so rapidly that the separation of niches on the substrate that characterises regime II approaches the width of a single stem [20].

Due to the complex behaviour of PEO during thermally-induced phase transitions novel experimental approach may yield additional information and make it possible to gain an insight into the course of melting and crystallisation—hence, in the step-scan alternating differential scanning calorimetry (SSA-DSC) the total heat flow is taken to be the average of the heat flow response to the heat-hold temperature program. In this way, the total heat flow can be separated into the reversing and non-reversing components, because the reversing component is only observed on the heating part of the cycle and the non-reversing only on the isothermal. There is no Fourier transformation for deconvolution of the traces, no curve substraction as the non-reversing response is directly extracted from the isothermal response and no phase lag component to the analysis [21].

In the present paper we report on the phase behaviour of a well-defined PEO (in terms of molecular weight characterisation) under step-scan temperature conditions when three main measurements parameters of the SSA-DSC were systematically varied.

2. Experimental

2.1. Materials

Poly(ethylene oxide) (PEO) was produced by Polysciences Co., Warrington, PA, USA. Molecular weight was determined by GPC performed at 40 °C on a Hewlett-Packard 1050 GPC System with a refractometric detector, using Shodex OH-Pac SB803 HQ 8 × 300 mm column from Showa Denko. DMF was used as the eluent at a flow rate of 0.7 $cm^3\ min^{-1}$, and sample concentration was 1% m/v. GPC data were processed using a GRAMS/386 program (Galactics) to calculate average molecular weights, $M_n = 9630$ and $M_w = 13,060$ as well as polydispersity coefficient, $M_w/M_n = 1.38$. Degree of crystallinity (X_c) was calculated using a formula

$$X_c = \frac{\Delta H - \Delta H_a}{\Delta H_m^0} = \frac{\Delta H_m}{\Delta H_m^0}$$

where: ΔH_m^0—heat of melting of 100% crystalline polymer (196.8 J/g) [22], ΔH_m—heat of melting of polymer under investigation, determined by differential scanning calorimetry (DSC). For the DSC measurements a Netzsch DSC 200, operating in a dynamic mode, was employed. Sample of ca. 4 mg weight was placed in sealed aluminium pan. The heating rate of 10 K/min was applied. Argon was used as an inert gas with flow rate 30 cm^3/min. Prior to use the calorimeter was calibrated with mercury and indium standards; an empty aluminium pan was used as reference. ΔH_m was measured as 180.6 J/g and the degree of crystallinity was calculated as 0.92. A crystalline PEO phase was additionally confirmed by FTIR method (Bio-Rad FTS 165 spectrometer, KBr pellets, resolution 4 cm^{-1}) by the presence of the triplet peak of the COC stretching vibration at 1153, 1106 and 1061 cm^{-1} with a maximum at 1106 cm^{-1} [23].

2.2. Technique

Thermal investigations were performed by using a Perkin–Elmer Pyris Diamond DSC. Measurements were done in closed aluminium pans with sample mass of 8 mg under argon flow of 20 cm^3/min. Prior to use the calorimeter was calibrated with indium standard.

The measurements' conditions are summarised in Table 1.

Table 1
The measurements' conditions

No.	t_{iso} [s]	b [K/min]	Step [deg]
1	30	2	0.25
2	30	2	0.5
3	30	2	1
4	48	2	0.25
5	48	2	0.5
6	48	2	1
7	60	2	0.25
8	60	2	0.5
9	60	2	1
10	48	1	0.5
11	48	0.5	0.5
12	48	0.25	0.5

2.3. Theory of MT-DSC

Modulated temperature differential scanning calorimetry (MT-DSC) is a relatively new technique that offers extended temperature profile capabilities by e.g. sinusoidal wave superimposed to the normal linear temperature ramp

$$T = T_0 + \beta t + B\sin(\omega t) \tag{1}$$

Where T is the program temperature, T_0 is the starting temperature, β is the underlying average heating rate, B is the amplitude of the temperature modulation, and $\omega = 2\pi/p[1/s]$, is the modulation angular frequency.

The superimposition may be also in form of oscillations, dynamic-isothermal heating and cooling segments, 'saw-tooth' profile, etc.

The equation to describe heat flow is derived from a simple equation based on thermodynamic theory in which

$$\mathrm{d}Q/\mathrm{d}t = C_{\mathrm{pt}}\mathrm{d}T/\mathrm{d}t + f(t,T) \tag{2}$$

where Q is the amount of heat absorbed by the sample, C_{pt} is the thermodynamic heat capacity, $f(t,T)$ is some function of time and temperature that governs the kinetic response of any physical or chemical transformation [24].

By assuming that the temperature modulation is small and that over the interval of the modulation the response of the rate of the kinetic process to temperature can be approximated as linear, one can rewrite Eq. (2) as

$$\frac{\mathrm{d}Q}{\mathrm{d}t} = C_{\mathrm{pt}}(\beta + B\omega\cos(\omega t)) + f'(t,T) + \Psi\sin(\omega t) \tag{3}$$

Where $f'(t,T)$ is the average underlying kinetic function once the effect of the sine wave modulation has been subtracted, Ψ is the amplitude of the kinetic response to the sine wave modulation and $(\beta + B\omega\cos(\omega t))$ is the measured quantity $\mathrm{d}T/\mathrm{d}t$.

Kinetic approach is based on differentiating between fast responses (equilibrium behaviour) and slower kinetically hindered processes including irreversible processes.

Eq. (3) can only be transformed into Eq. (4) if one assumes that the system response is fast enough such that equilibrium is maintained during temperature changes [25]

$$\Phi(T(t)) = \Phi_{\mathrm{dc}}(T(t)) + \Phi_{\mathrm{a}}(T(t))\cos(\omega_0 t - \varphi) \tag{4}$$

where φ is the phase shift, Φ_{a} the cyclic component, Φ_{dc} the underlying heat flow.

We obtain the reversing component of the heat flow from

$$\Phi_{\mathrm{rev}}(T(t)) = \frac{\Phi_{\mathrm{a}}(T(t))}{B\omega_0}\beta_0 \tag{5}$$

The kinetic component (the non-reversing component) is then

$$\Phi_{\mathrm{non}}(T(t)) = \Phi_{\mathrm{dc}}(T(t)) - \Phi_{\mathrm{rev}}(T(t)) \tag{6}$$

The modulated temperature and resultant modulated heat flow can be deconvoluted using a Fourier transform to give reversing and non-reversing components. The reversing component is evaluated from the periodic part of the heat flow. The non-reversing component is the difference between the underlying heat flow (static heat flow) and the reversing component. The static heat flow is evaluated by an averaging method. Amplitude of the cyclic response and the phase lag are divided into in and out of phase responses by use of the phase lag unless the phase shift is small in which case the out of phase component can be neglected [26].

An alternative evaluation method has been reported based on the linear response approach [27]. In this method, the heat flow into the sample is described as

$$\Phi(t) = \int_0^t C(t-\tau)\beta(\tau)\mathrm{d}\tau \tag{7}$$

with

$$\beta(t) = \beta + \omega_0 B\cos(\omega_0 t) \tag{8}$$

where C is complex heat capacity.

Insertion of Eq. (8) into Eq. (7) and integration leads to the relationship

$$\Phi(T(t)) = C_\beta(T)\beta + \omega B|C(T,\omega)|\cos(\omega t - \varphi) \tag{9}$$

with

$$|C| = \sqrt{C'^2 + C''^2} \tag{10}$$

Where C' is the storage heat capacity (associated with mobility); C'' is the loss heat capacity (associated with dissipation).

Both the phase shift and the amplitude of the dynamic component are used for the calculation of a complex (frequency-dependent) heat capacity. These quantities can be interpreted in the context of the relaxation theory or irreversible thermodynamics [25].

In the step-scan alternating DSC, the temperature program comprises a periodic succession of short, heating rates and isothermal steps; the measured heat flow contains thus contributions which arise from the heat capacity and those due to physical transformations or chemical reactions. The non-reversing heat flow is the change in heat flow that occurs during the isothermal segment of the heat-hold experiment and the total heat flow is taken to be the average of the heat flow response to the heat-hold temperature program. In this way, the total heat flow can be separated into the reversing and non-reversing components, because the reversing component is only observed on the heating part of the cycle and the non-reversing only on the isothermal. Since both the heat capacity equilibration and DSC equilibration are rapid, the C_{p} calculation is said to be independent of kinetic processes [21].

Since there is no complex Fourier transform involved in data deconvolution and no phase lag component to the analysis, the reported advantages include reliable and direct heat capacity measurement with low mass samples over a

much shorter time than experiments performed in equivalent large mass heat flux modulated temperature DSC.

3. Results and discussion

Influence of the three main measurement's parameters of SSA-DSC method: length of the isothermal segment (t_{iso}/s), temperature jump between two subsequent isothermal segments (step/deg) and linear heating rate in dynamic segments (b/K/min), on the shape of reversing and non-reversing components during the melting and crystallisation of PEO, has been evaluated.

3.1. Influence of the length of the isothermal segment

Results of the SSA-DSC measurements for $t_{iso} = 30$, 48 or 60 s are exhibited in Fig. 1.

For longer isothermal segments a decrease in the change of enthalpy of transition can be observed for both melting and crystallisation. By increasing the isothermal time better conditions for recrystallisation (in the melting region) and partial melting (for crystallisation) are created and the total heat flow is therefore lower.

More information can be obtained if reversing and non-reversing components are separated for the melting process— Figs. 2 and 3.

It can be seen that the reversing component during melting of PEO is increasing with an increase of the isothermal segment length. This effect is due to the existence of defected polymer crystal structures that form metastable regions between crystal phase and already melted polymer. Reversible recrystallisation in the presence of still existing polymer crystals is facilitated by longer isothermal segments. A quasi-isothermal MTDSC experiment in the melting region can be separated into an initial non-isothermal step and the quasi-isothermal measurement; during the measurement at the initial stage the sample state relaxes into a meta-stable equilibrium. Reversible melting in quasi-isothermal step consists of real reversible melting

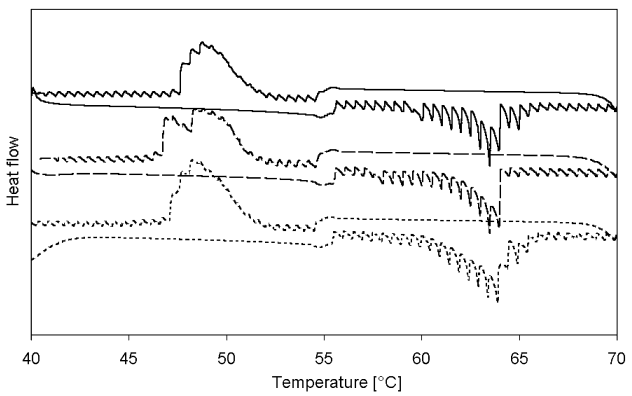

Fig. 1. SSA-DSC profiles of PEO at different t_{iso} (step = 0.5 deg., $b = 2$ K/min): 30 s (dotted line), 48 s (dashed line), 60 s (full line).

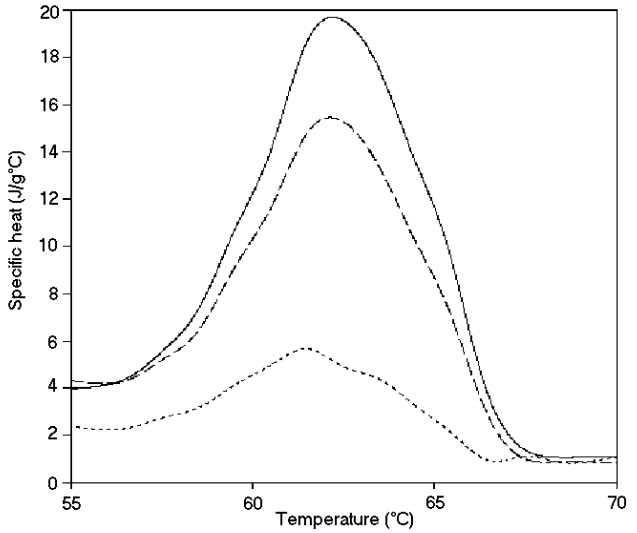

Fig. 2. SSA-DSC reversing component of the melting process of PEO at different t_{iso} (step = 1 deg., $b = 2$ K/min): 30 s (dotted line), 48 s (dashed line), 60 s (full line).

of crystals and reorganisation to crystals with a higher stability and characterised by higher melting temperature occurrs. The reorganisation of the crystals can be understood as a structural relaxation of native crystals into equilibrium crystals [28,29].

Distortions of the signal shape in the melting region were observed—they are probably caused by differences in the kinetics of melting and recrystallisation which may have different degrees of reversibility. Reversible melting is due to local equilibria of flexible chain segments within a metastable phase structure; poorer crystals show diffusional effects [30,31].

Non-reversing component shows different behaviour—if isothermal segments are long enough, thermodynamically-driven recrystallisation occurs; for shorter iso times kinetically-controlled non-reversing processes with lower activation energy barrier are prevailing.

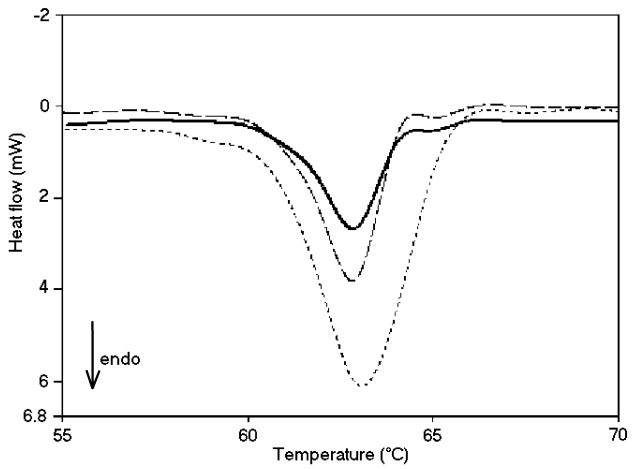

Fig. 3. SSA-DSC non-reversing component of the melting process of PEO at different t_{iso} (step = 1 deg., $b = 2$ K/min): 30 s (dotted line), 48 s (dashed line), 60 s (full line).

Oscillating DSC was applied by Alden et al. [32] to investigate the heat of fusion of PEO with average molecular weight 6000, using a series of combinations of frequency, amplitude and underlying heating rate. They observed that the selection of variables did not significantly influence the conventional heat of fusion values, but had an impact on the values of the reversible C_p component and the irreversible kinetic component; during melting, an increased heating rate or amplitude broadened the melting interval whereas an increased frequency narrowed it. The changes can be related to the real heating rate accomplished by the oscillation and to the effect of the oscillation temperature history on the crystallisation process.

Similar trend, although not so clearly visible due to more complex behaviour of a system during solidification, was observed in the crystallisation region, as it is shown in Fig. 4 (reversing component) and Fig. 5 (non-reversing component).

Longer isothermal segments enable reversible partial nucleation which in turn lead to an increase in the specific heat. For the non-reversing component the rate of partial recrystallisation processes becomes a dominating factor.

3.2. Influence of the temperature jump between two subsequent isothermal segments

An increase of the temperature step between subsequent isothermal segments increases the total heat flow for both melting and crystallisation, as seen in Fig. 6.

By increasing the step, the equilibrium of reversible processes is shifted towards products and activation of rate-controlled processes takes place; chain nucleation is hampered and partial melting and/or recrystallisation proceed slower—this effect can be observed as a decrease of reversing signal with increasing step, as seen in Fig. 7 (peak area at step: 1 deg.—143.1; 0.5 deg.—190.4; 0.25 deg.—266.2 [J/g °C min]).

Melting and crystallisation of flexible macromolecules under temperature modulated program is a sequence of events which involve equilibrium developed by diffusion of selected fractions to the surfaces of the remaining crystals, whereby diffusion of other crystal forms is hindered [33,34].

Signal describing the non-reversing component of the heat flow during melting (Fig. 8) is increasing with an increase of step which is due to overcoming of the activation

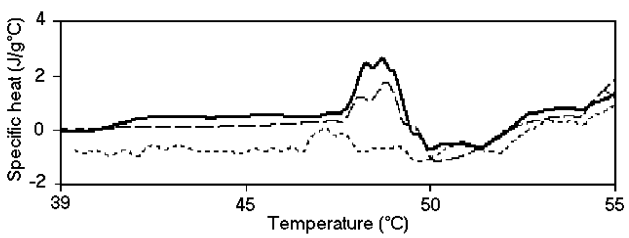

Fig. 4. SSA-DSC reversing component of the crystallisation process of PEO at different t_{iso} (step = 0.25 deg., b = 2 K/min): 30 s (dotted line), 48 s (dashed line), 60 s (full line).

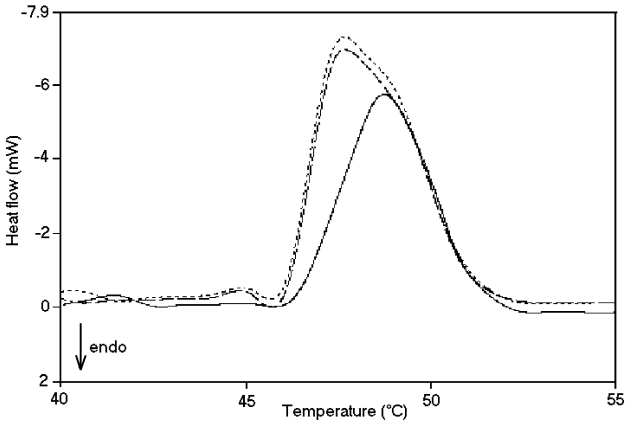

Fig. 5. SSA-DSC non-reversing component of the crystallisation process of PEO at different t_{iso} (step = 1 deg., b = 2 K/min): 30 s (dotted line), 48 s (dashed line), 60 s (full line).

barrier by more partial sub-processes that originate from the phase transition of different-size crystal arrangements-less stable folded-chain crystallites of PEO undergo melting at a lower temperature than extended chain crystals which are located preferentially at the spherulite interface whereby single crystals are flat platelets, known as lamellae and are arranged in spherical structures—spherulites. Various types of PEO morphology between two extreme cases of the extended-chain crystal and the folded-chain crystal cause a complex phase transition behaviour.

During the crystallisation process of PEO at different step, reversing component shows a perturbed behaviour (Fig. 9) since non-reversing processes dominate; the latter depend on measurement (external) conditions in such a way that higher step facilitates nucleation and subsequent crystallisation during the next iso segment as seen in Fig. 10.

A semi-crystalline polymer has a non-equilibrium structure. During heating in conventional DSC melting and recrystallisation effects can be observed simultaneously. Both the structure of the crystals and of the melt depends on the temperature. In addition to imperfect crystals and a re-ordered melt, a semi-crystalline polymer

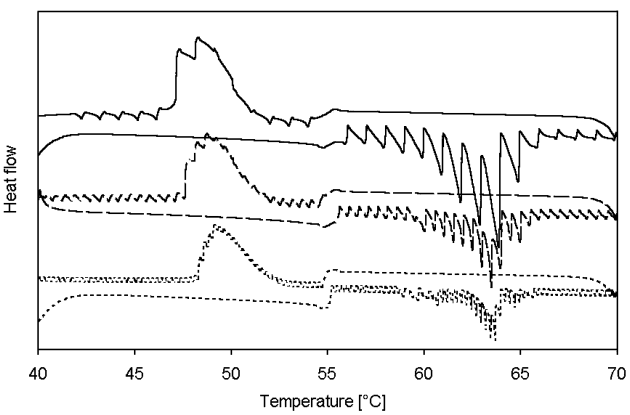

Fig. 6. SSA-DSC profiles of PEO at different temperature jumps between two subsequent isothermal segments: 0.25 deg. (dotted line), 0.5 deg. (dashed line), 1 deg. (full line).

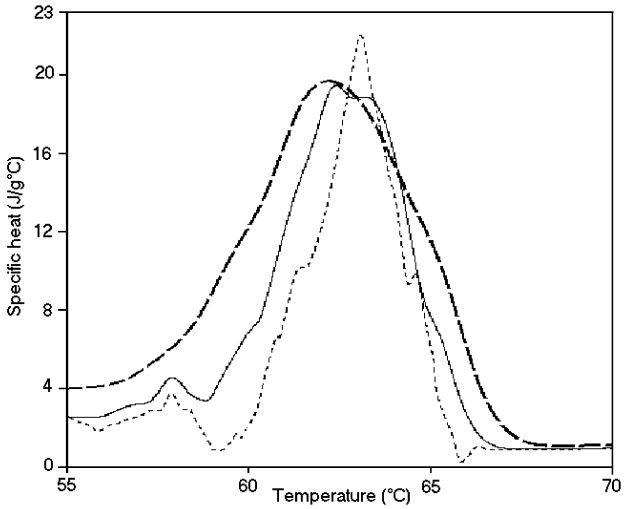

Fig. 7. SSA-DSC reversing component of the melting process of PEO at different step ($t_{iso} = 60$ s, $b = 2$ K/min): 0.25 deg. (dotted line), 0.5 deg. (dashed line), 1 deg. (full line).

includes a rigid amorphous phase on the surface of the crystallites.

In a quasi-isothermal mode of MT-DSC measurement, the sample response during a small periodic (in terms of amplitude and period) temperature perturbation is measured as a function of time. In the initial step, the state of the sample becomes a (stationary) non-equilibrium. For the physical explanation of the relaxation processes a model function was proposed, which assumes that the isothermal relaxation process during melting is mainly influenced by irreversible melting of the crystals (the volume fraction which shows reversible effects decreases during the measurement). The causes for the decrease of the relevant volume fraction of the crystals can be both real reversible melting of crystals and/or re-organisation process leading to crystals with a higher stability (higher melting temperature). The re-organisation process can be understood as a structural relaxation of native crystals into equilibrium

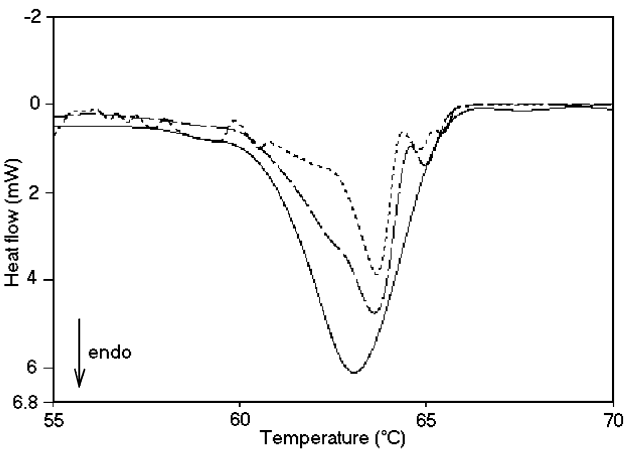

Fig. 8. SSA-DSC non-reversing component of the melting process of PEO at different step ($t_{iso} = 30$ s, $b = 2$ K/min): 0.25 deg. (dotted line), 0.5 deg. (dashed line), 1 deg. (full line).

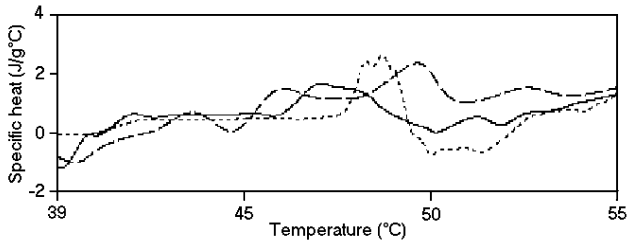

Fig. 9. SSA-DSC reversing component of the crystallisation process of PEO at different step ($t_{iso} = 60$ s, $b = 2$ K/min): 0.25 deg. (dotted line), 0.5 deg. (dashed line), 1 deg. (full line).

crystals. In a quasi-isothermal mode of MT-DSC measurement, the sample response during a small periodic temperature perturbation is measured as a function of time. In the initial step, the state of the sample becomes a (stationary) non-equilibrium. For the physical explanation of the relaxation processes a model function was proposed:

$$|c| = \sqrt{c_i^2 + B_1 t_m^{-0.5} + B_2 t_m^{-1}} \tag{11}$$

Where $|c|$ complex heat capacity, t_m is the measuring time, parameters $B_1 = 2(c_{st}A_1 + c_2A_2)$ and $B_2^2 = A_1^2 + A_2^2$, $c_i^2 = c_{st}^2 + c_2^2$ (A_1, A_2 depend on the averaged superheating, c_{st} is the static specific heat of the meta stable equilibrium, c_2 is a constant).

Its physical meaning is that the isothermal relaxation process during melting is mainly influenced by irreversible melting of the crystals [29].

3.3. Influence of the heating rate

Heating rate plays an important role during the thermal analysis experiment—similarly, it influences considerably the shape of heat flow curve under step scan condition, as seen in Fig. 11.

If a heating rate increases, reversing signal for the

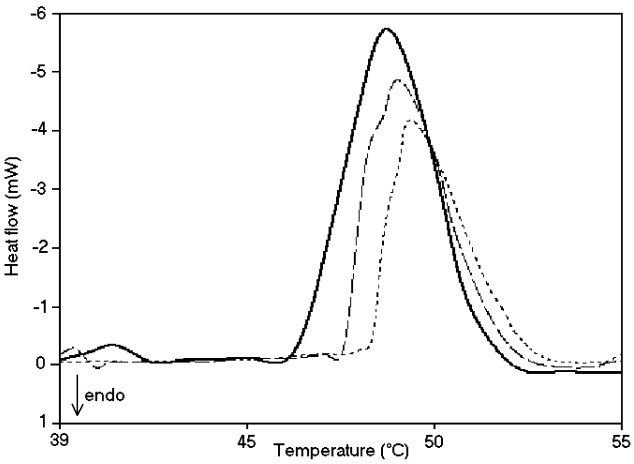

Fig. 10. SSA-DSC non-reversing component of the crystallisation process of PEO at different step ($t_{iso} = 60$ s, $b = 2$ K/min): 0.25 deg. (dotted line), 0.5 deg. (dashed line), 1 deg. (full line).

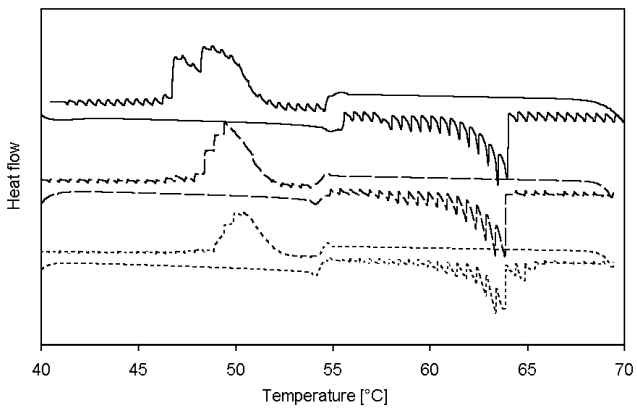

Fig. 11. SSA-DSC profiles of PEO at different heating rate; $t_{iso} = 48$ s, step = 0.5 deg.: 0.5 K/min (dotted line), 1 K/min (dashed line), 2 K/min (full line).

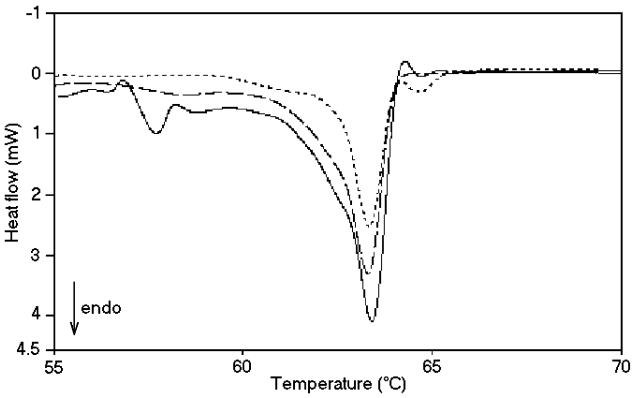

Fig. 13. SSA-DSC non-reversing component of the melting process of PEO at different heating rates ($t_{iso} = 48$ s, step = 0.5 deg.): 0.5 K/min (dotted line), 1 K/min (dashed line), 2 K/min (full line).

melting process becomes smaller due to induced restrictions for recrystallisation, as seen in Fig. 12.

Rate-controlled processes constitute a growing part of the total heat flow for measurements with increasing heating rate, as evidenced in Fig. 13.

Imaginary part of the complex heat capacity shows strong frequency dependence and it represents the temperature coefficient of the total heat flow in the transformation region which carries the information about the time-dependent kinetics of the transformation.

The crystallisation behaviour of PEO at different heating rates is characterised by perturbed course of the reversing component, as seen in Fig. 14.

Fig. 15 presents a changing profile of non-reversing part; it increases with an increase of the heating rate.

One should note that at the highest heating rate there is a double-peak which may originate from different crystallisation patters of PEO fractions.

The nature of recrystallisation related to metastability of polymer crystals is an important issue that influences warp, dimensional stability, creep, softening and heat deflection temperature. On the processing side, high-temperature coalescence and adhesion are crucial in the solid state polymerisation. Sauer et al. [35] used MT-DSC technique to characterise melting and recrystallisation of poly(oxy-1,4-phenyleneoxy-1,4-phenylenecarbonyl-1,4-phenylene) (PEEK)—for the interpretation of MT-DSC results three main rules have been applied: (i) the non-reversing endothermic signal is typically due to complete melting of separate lamellae or stacks of lamellae; sometimes perfected crystals cannot recrystallise fast enough because of a low degree of undercooling, (ii) the reversing endothermic signal is due to partial melting of lamellae which are then able to recrystallise quite rapidly due to templating of the just melted chains as they recrystallise on existing crystals (the physics of this process was discussed in detail in Ref. [36]) and, (iii) crystallisation exotherms contribute only to the non-reversing signal which is used for separation of exotherms from e.g. reversible melting.

It has already been shown by comparison of quasi-isothermal MT-DSC of a quickly and a slowly cooled sample of PEO that the better crystals (extended-chain crystals) show smaller amount of reversing melting, and on cooling an identical reversing heat capacity as obtained on

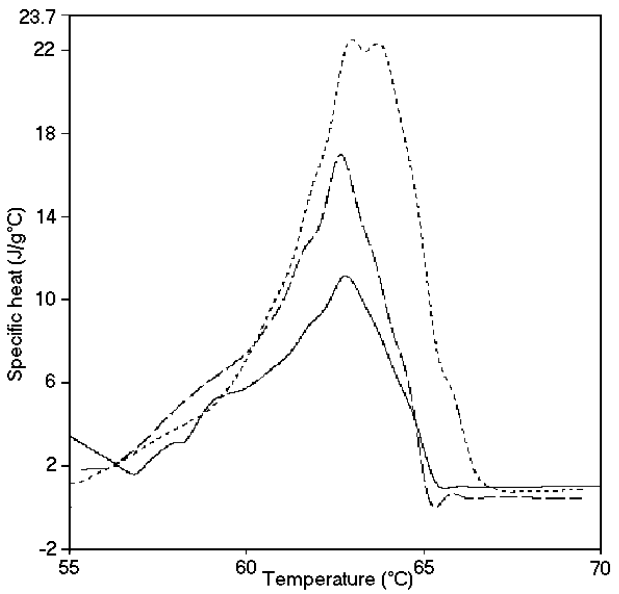

Fig. 12. SSA-DSC reversing component of the melting process of PEO at different heating rates ($t_{iso} = 48$ s, step = 0.5 deg.): 0.5 K/min (dotted line), 1 K/min (dashed line), 2 K/min (full line).

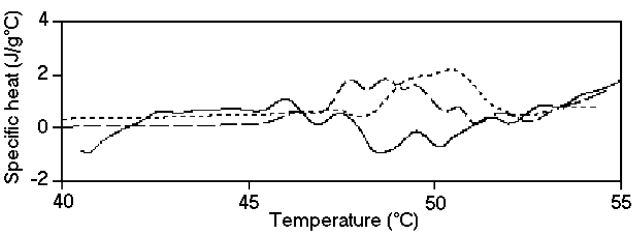

Fig. 14. SSA-DSC reversing component of the crystallisation process of PEO at different heating rates ($t_{iso} = 48$ s, step = 0.5 deg.): 0.5 K/min (dotted line), 1 K/min (dashed line), 2 K/min (full line).

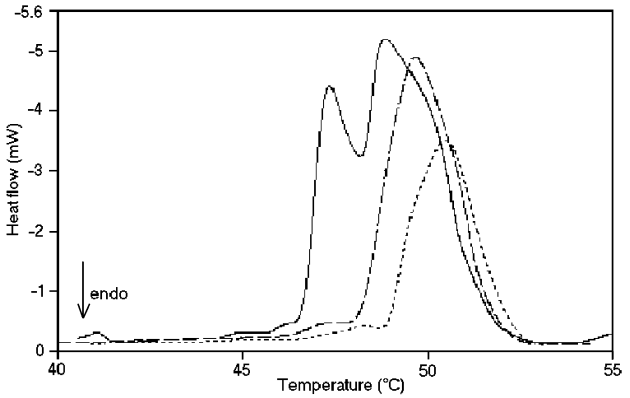

Fig. 15. SSA-DSC non-reversing component of the crystallisation process of PEO at different heating rates (t_{iso} = 48 s, step = 0.5 deg.): 0.5 K/min (dotted line), 1 K/min (dashed line), 2 K/min (full line).

heating is recovered [37]. Results of these experiments indicate two different origins of the increase of heat capacity—one is due to beginning of creation of conformational defects above the glass transition and the other is caused by reversing melting [30].

Simultaneously, the reversing apparent heat capacity shows a complex behaviour and depends on a series of events that include melting of poor crystals, recrystallisation and diffusional effects of the crystallising species; finally, a steady state is established that shows a higher level of reversible melting and crystallisation than in the beginning [34,38].

The MT-DSC signal made it possible to explain that the 'low endotherm', routinely detected by standard DSC a few degrees above isothermal annealing temperatures, is probably a superimposition of early melting of secondary crystals with almost simultaneous exothermic recrystallisation.

4. Conclusions

Step scan alternating DSC proved to be a useful method to characterise the phase transitions of poly(ethylene oxide)—melting and crystallisation—by separating the reversing and non-reversing components of the heat flow. It has been found that the reversing component during melting of PEO is increasing with an increase of the isothermal segment length. This effect is due to the existence of defected polymer crystal structures that form metastable regions between crystal phase and already melted polymer. Reversible re-crystallisation in the presence of still existing polymer crystals is facilitated by longer isothermal segments. By increasing the step, the equilibrium of reversible processes is shifted towards products and activation of rate-controlled processes takes place; chain nucleation is hampered and partial melting and/or re-crystallisation proceed slower—this effect can be observed as a decrease of reversing signal with increasing step. The crystallisation behaviour of PEO at different heating rates is characterised by perturbed reversing component and changing profile of non-reversing part that increases with an increase of the heating rate. One should note that at the highest heating rate there is a double-peak which may originate from different crystallisation patters of PEO fractions.

Acknowledgements

Authors are grateful to the Polish Committee for Scientific Research (grant No PB 0975/T09/2002/22) for financial support.

References

[1] Bailey JrFE, Koleske JV. Poly(ethylene oxide). New York: Academic Press; 1976.
[2] Craig DQM. Thermochim Acta 1995;248:189.
[3] Acosta JL, Morales EJ. J Appl Polym Sci 1996;60:1185.
[4] Mastragostino M, Arbizzani C, Meneghelo L, Paraventi R. Adv Mater 1996;4:331.
[5] De Paoli MA, Zanelli A, Mastragostino M, Rocco AM. J Electroanal Chem 1997;435:217.
[6] Rocco AM, Bielschowsky CE, Pereira RP. Polymer 2003;44:361.
[7] Babich MW, Benrashid R, Mounts RD. Thermochim Acta 1994;243:193.
[8] Pielichowski K, Flejtuch K. Polym Adv Technol 2002;13:690.
[9] Takahashi Y, Tadokoro H. Macromolecules 1973;6:672.
[10] Cheng SZD, Barley JS, Giusti PA. Polymer 1990;31:845.
[11] Avrami MJ. J Chem Phys 1941;9:177.
[12] Lauritzen Jr. JI, Hoffman JD. J Appl Phys 1973;44:4340.
[13] Hoffman JD, Miller RL. Macromolecules 1988;21:3038.
[14] Godovsky YuK, Slonimsky GL, Garbar NM. J Polym Sci Part C 1972;38:1.
[15] Kovacs AJ, Straupe C, Gonthier A. J Polym Sci Polym Symp 1977;59:31.
[16] Kovacs AJ, Straupe C. J Chem Soc Faraday Discuss 1979;68:225.
[17] Kovacs AJ, Straupe C. J Cryst Growth 1980;48:210.
[18] Cheng SZD, Chen J, Heberer DP. Polymer 1992;33:1429.
[19] Wu L, Lisowski M, Talibuddin S, Runt J. Macromolecules 1999;32:1576.
[20] Ding N, Amis EJ. Macromolecules 1991;24:3906.
[21] Sandor M, Bailey NA, Mathiowitz E. Polymer 2002;43:279.
[22] Wunderlich B. Thermal Analysis. San Diego: Academic Press; 1990.
[23] Li X, Hsu SL. J Polym Sci Polym Phys Ed 1984;22:1331.
[24] Reading M, Luget A, Wilson R. Thermochim Acta 1994;238:295.
[25] Schawe JEK, Hőhne GWH. Thermochim Acta 1996;287:213.
[26] Reading M. Trend Polym Sci 1993;1:248.
[27] Schawe JEK. Thermochim Acta 1995;260:1.
[28] Schmidtke J, Strobl GR, Thurn-Albrecht T. Macromolecules 1997;30:5804.
[29] Schawe JEK, Winter W. Thermochim Acta 1999;330:85.
[30] Wunderlich B. Prog Polym Sci 2003;28:383.
[31] Schawe JEK, Bergmann E, Winter W. J Therm Anal 1998;54:565.
[32] Alden M, Wulff M, Herdinius S. Thermochim Acta 1995;265:89.
[33] Hutchinson JM, Monserat S. Thermochim Acta 1996;286:263.
[34] Ishikiriyama K, Wunderlich B. Macromolecules 1997;30:4126.
[35] Sauer BB, Kampert WG, Blanchard EN, Threefoot SA, Hsiao BS. Polymer 2000;41:1099.
[36] Okazaki I, Wunderlich B. Macromol Rapid Commun 1997;18:313.
[37] Hu WB, Albrecht T, Strobl G. Macromolecules 1999;32:7548.
[38] Ishikiriyama K, Wunderlich B. J Polym Sci Part B Polym Phys 1997;35:1877.